Crashworthiness Optimization of Tubular Structures

氏　　　　名	韓　　　　晶
生 年 月 日	
本　　　　籍	中国
学 位 の 種 類	博士（工学）
学 位 記 番 号	博甲第301号
学位授与の日付	平成11年3月25日
学位授与の要件	課程博士（学位規則第4条第1項）
学位授与の題目	Crashworthiness Optimization of Tubular Structures（薄肉構造部材の衝撃圧潰特性最適化に関する研究）
論 文 審 査 委 員	（主　査）山崎　光悦
	（副　査）尾田　十八，放生　明廣，前川　幸次，桝谷　　浩

学 位 論 文 要 旨

The dissertation deals with the development of the crashworthiness optimization technique for tubular structures by using the Response Surface Methodology. In the proposed system, an orthogonal array in the Orthogonal Factorial Experimental Design is employed to assign analysis points, and the nonlinear dynamic finite element code, DYNA3D, is adopted to simulate the complicated impact crushing behavior of tubular structures at each analysis point. Based on the numerical results in the pre-assigned design space, the approximated response surface of the structural behavior is constructed in the form of orthogonal polynomial which is then optimized by using the usual mathematical programming technique. This optimization process is repeated until the given convergence conditions are satisfied. The optimization system has been applied to maximize the absorbing energy of cylindrical tubes, unstiffened and stiffened square tubes as well as S-Shape square tubes under axial impact condition.

1. Introduction

Tubular structures are known to be efficient absorbers to the kinetic energy of moving bodies, therefore, investigation of crashworthiness optimization of tubular structures is very important and is expected from the point of view of safety design of passenger vehicles. In order to reduce the damage to occupants in a collision, it is necessary to understand the crush behavior and to enhance the energy absorption capability of tubular structures. This dissertation deals with the development of crashworthiness optimization technique for tubular structures by using the response surface methodology. The optimization system has been applied to maximize absorbing energy of cylindrical tubes, unstiffened and stiffened square tubes as well as S-shape square tubes subjected to axial impact loads.

2. Dynamic Response of Tubular Structures

2.1 Numerical Simulation As an example, the dynamic response of a cylindrical tube impacted against a rigid wall at an initial velocity $V_0 = 10\mathrm{m/s}$, as shown in Fig. 1, is studied by using the nonlinear dynamic finite element code, DYNA3D. Several kinds of models of mean radius *R*, mean wall thickness *H* and initial axial length L are analyzed. A mass is attached to the one end of the cylinder in order to supply enough energy for crushing. The added mass weight is 500 times the cylinder weight. The analysis time step $\triangle t$ is decided automatically depending on the finite element divisions.

Figure 2 shows three kinds of typical crushing deformation patterns of three models having the same mass (0.53 kg) but different dimensions. In pattern (a), five axisymmetric wrinkles appeared. Model (b) developed an initial circular wrinkle followed by a triangle and then by a pentagon. This pattern shift from axisymmetric to non-axisymmetric is due to the change of the ratio R/H. Column buckling occurred in model (c).

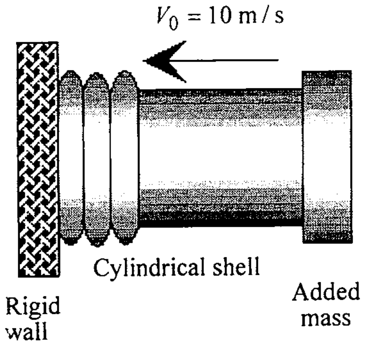

Fig.1 Analysis and design model.

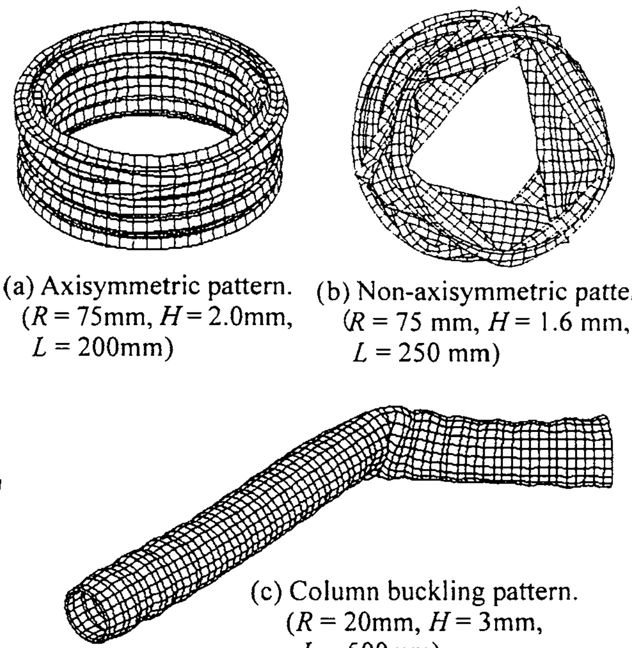

(a) Axisymmetric pattern. ($R = 75$mm, $H = 2.0$mm, $L = 200$mm)

(b) Non-axisymmetric pattern. ($R = 75$ mm, $H = 1.6$ mm, $L = 250$ mm)

(c) Column buckling pattern. ($R = 20$mm, $H = 3$mm, $L = 500$mm)

Fig. 2 Typical crushing deformations of cylindrical tube.

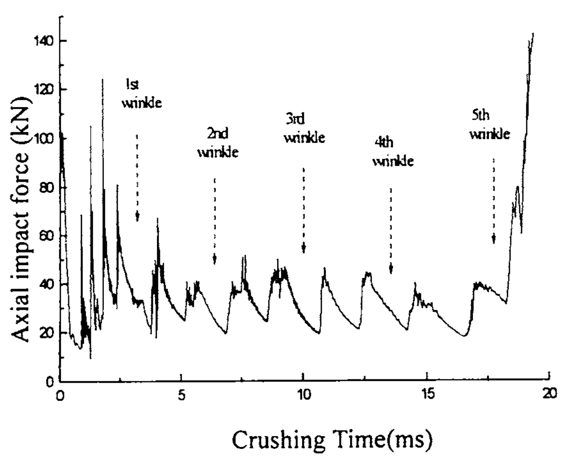

Fig. 3 Axial force - crushing time curve of model (a).

Figure 3 shows the axial crushing force-time curve of model (a). Analyzing the curve, we can observe that during the formation of the first wrinkle there are several force peaks, and during the formation of subsequent wrinkles there are two force peaks in the force-time diagram. The last high peak appears after the cylinder bottoms out. The total absorbing energy in progressive buckling is defined as the total energy absorbed just before the cylinder bottoms out, which is about 5.3 kJ and 4.8 kJ in the cases of (a) and (b), respectively. The energy absorbed by model (c), 2.7 kJ, is much less than that of the progressive buckling models because energy absorption ceased after column buckling occurred.

2.2 Experimental Validation For the experimental validation of the FE analysis, a series of aluminum cylindrical shells were tested under axial impact condition. The cylindrical specimen attached a mass was accelerated under the recovery force of the rubber stretched by a winch. The dynamic deformation process was photographed by using a high speed video camera. Two pairs of speed sensors are equipped to record the axial impacting and reflecting velocities as shown in Fig. 4. The comparison results shows that the impact behavior is simulated reasonably well by the FEM described above. Therefore, it is reasonable to use explicit FE analysis to maximize the absorbing energy.

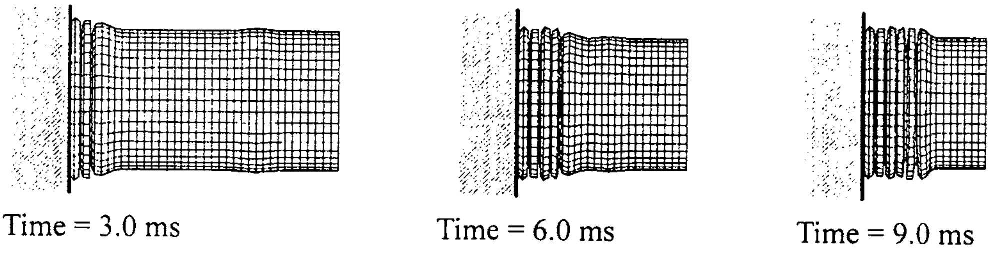

(a) Numerical simulation by DYNA3D.

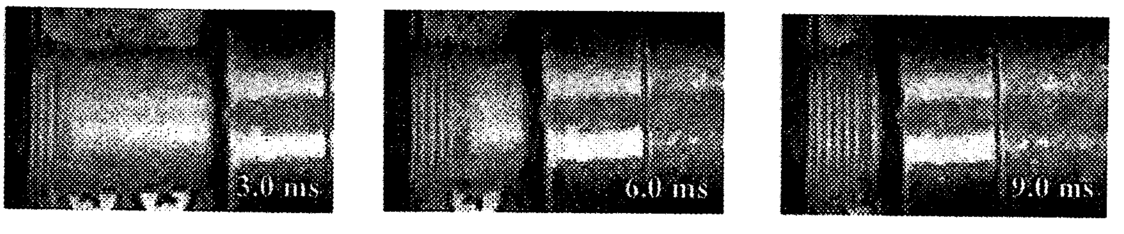

(b) Experimental results.

Fig. 4 Impact crushing deformation.

3. Maximization Technique of the Absorbing Energy

Few papers have been published on the maximization technique of the crushing energy absorption. This paper proposes a new numerical method to maximize the absorbing energy for tubular structures. Suppose design variables are denoted by

$$\mathbf{X}^T = \{x_1, x_2, ..., x_{nd}\}, \tag{1}$$

where n_d is the number of design variables, the maximization problem of the crushing energy absorption of tubular structures can then be stated as

$$f = U(\mathbf{X}) \rightarrow \max \tag{2}$$

subject to the mean axial impact force P_m and the upper and lower bounds of the design variables as

$$g = P_m / P_{ma} - 1 \leqq 0 \tag{3}$$

$$x_{n\,\min} \leqq x_n \leqq x_{n\,\max},\ n = 1, 2, ..., n_d \tag{4}$$

where U and P_{ma} denote the absorbing energy during crushing and the allowable limit of the mean axial impact crushing force, respectively. Figure 5 shows the flowchart of the optimization technique. An orthogonal array in the design-of-experiment is employed to assign analysis points, and the nonlinear dynamic finite element code, DYNA3D, is adopted to simulate the complicated impact crushing behavior of tubular structures at each analysis point. Based on the numerical results of the structural behavior, the response surface approximation technique is applied to generate an approximate function of the absorbing energy in terms of the design variables that are evaluated to be significant at high levels to the response by the analysis-of-variance. The approximate function of the absorbing energy is then maximized under the constraints of a constant volume and mean axial force by the numerical optimization program, DOT. This optimization process is repeated until the given convergence conditions are satisfied.

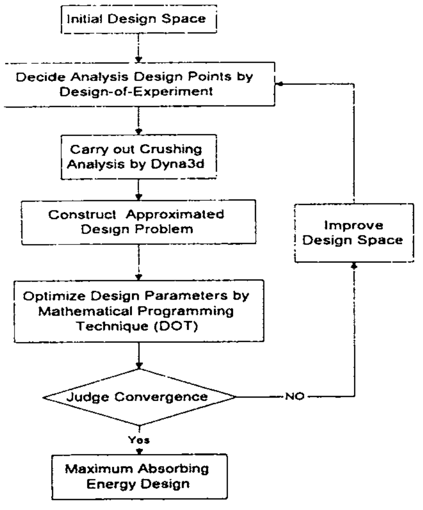

Fig. 5 Flowchart of maximization of absorbing energy.

Table 1 Numerical results in the 1st design cycle. (N : Non-axisymmetric wrinkle C: Circular wrinkle)

Design points	R mm	H mm	U kJ	P_m kN	Crushing pattern
1	50	2	6.98	25.95	4C+2N
2	75	2	5.31	31.63	5C
3	100	2	4.03	33.05	3C
4	50	3	8.35	51.12	4C
5	75	3	7.03	61.14	3C
6	100	3	5.52	67.40	2C
7	50	4	9.02	74.50	3C
8	75	4	8.05	99.15	2C
9	100	4	6.67	124.94	1C

4. Numerical Examples

The impact analysis model of the cylinder is the same as that described in Section 2.1. The radius and thickness of the cylindrical tube are taken as design variables while keeping the mass constant (0.53 kg). The mean axial force P_m is constrained less than $P_{ma} = 68.6$ kN. The upper and lower bounds of the design variables are also restricted in the initial design cycle as: 50.0 mm $\leqq R \leqq$ 100.0 mm, 2.0 mm $\leqq H \leqq$ 4.0 mm. Three design levels of each design variable have the same intervals, respectively. The results of the structural analysis are shown in Table 1 for 9 design points. The functions of the absorbing energy and the mean axial impact force are approximated by orthogonal polynomials as

$$\begin{aligned} U(R,H) = {} & 6.77 - 0.054\times(R-75.0) - 0.0001\times[(R-75.0)^2 - 416.67] \\ & + 1.24\times(H-3.0) - 0.29\times[(H-3.0)^2 - 0.67] \\ & + 0.006\times(R-75.0)\times(H-3.0) \end{aligned} \tag{5}$$

$$
\begin{aligned}
P_m(R,H) = {} & 63.21 - 0.492 \times (R-75.0) - 0.0018 \times [(R-75.0)^2 - 416.67] \\
& + 34.66 \times (H-3.0) + 4.98 \times [(H-3.0)^2 - 0.67] \\
& + 0.4334 \times (R-75.0) \times (H-3.0) \\
& + 0.0043 \times (R-75.0) \times [(H-3.0)^2 - 0.67] \\
& + 0.0002 \times [(R-75.0)^2 - 416.67] \times (H-3.0) \\
& + 0.0002 \times [(R-75.0)^2 - 416.67] \times [(H-3.0)^2 - 0.67]
\end{aligned}
\tag{6}
$$

Figure 6 shows the approximated response surface of the absorbing energy. The approximated subproblem is then solved by the feasible direction method. The optimum result of the initial design cycle is shown in Table 2 as design cycle 1. It is found that the design variable R coincides with the lower bound, and that the thicker the tube is, the more energy is absorbed. Therefore, the design space is then improved by reducing the radius R and increasing the thickness H for the second design cycle as: 20.0 mm $\leqq R \leqq$ 50.0 mm, 3.0 mm $\leqq H \leqq$ 5.0 mm. Figure 7 shows the approximated response surface of the absorbing energy in the second design cycle. From the numerical results in two design cycles for the pre-assigned design space, we can observe that the absorbing energy increases to a maximum point and then decreases suddenly and rapidly due to the column buckling with the ratio R/H decreasing, as shown in Fig. 8. It is evident that the absorbing energy response surface is not continuous because the column buckling occurs suddenly, hence, the response surface approximation technique gives a rough approximated response surface for a discontinuous problem. To obtain more precise approximated response surface, the range of the radius is narrowed in the third design cycle as: 20.0 mm $\leqq R \leqq$ 35.0 mm. Table 2 shows the optimization results in three design cycles by DOT. The optimized cylinder developed 6 axisymmetric progressive wrinkles as simulated in Fig. 9. The numerical estimates of the absorbing energy and mean axial impact force of the optimized cylinder are 11.5 kJ and 64.7 kN, respectively.

The proposed algorithm has also been applied to the absorbing energy maximization problems of unstiffened square tubes (Fig. 10) in which the mean width and mean wall thickness are selected as design variables, as well as axially stiffened square tubes (Fig. 11) in which the mean width and wall thickness of the

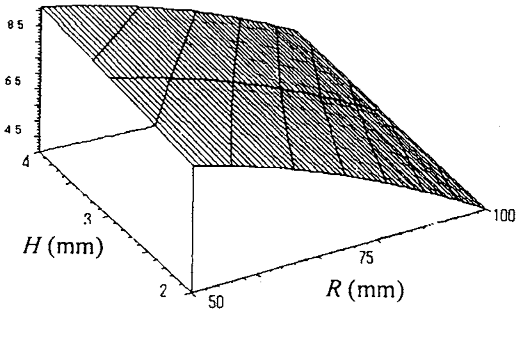

Fig. 6 Approximated response surface of absorbing energy in the 1st design cycle.

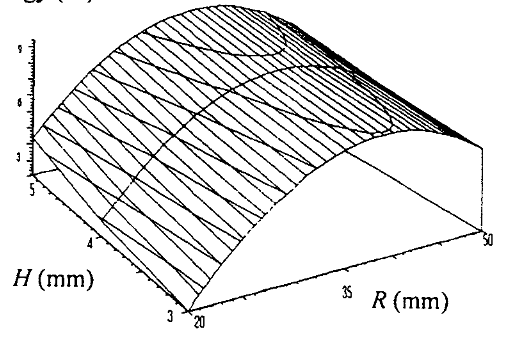

Fig. 7 Approximated response surface of absorbing energy in the 2nd design cycle.

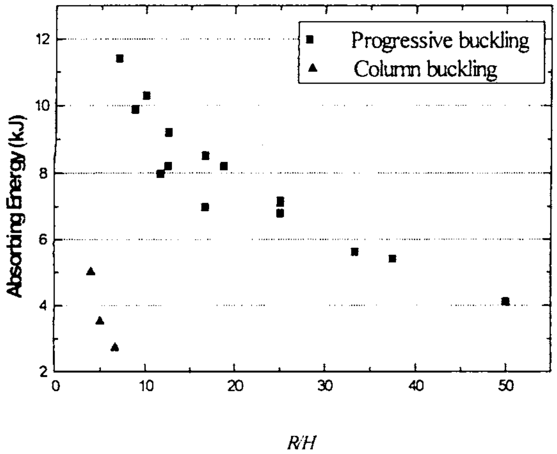

Fig. 8 Absorbing energy v.s. *R/H.*

Table 2 Optimization results by DOT.

Design Cycle	R mm	H mm	U kJ	g
1	50.0	3.78	8.98	2.00E-3
2	37.9	4.01	9.78	-2.37E-4
3	29.6	4.14	11.4	-2.20E-4

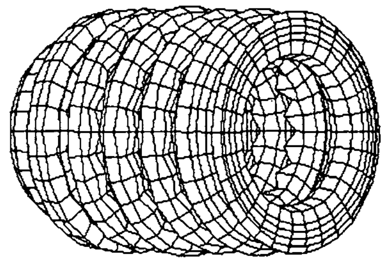

Fig. 9 Simulation of the optimized cylindrical tube.

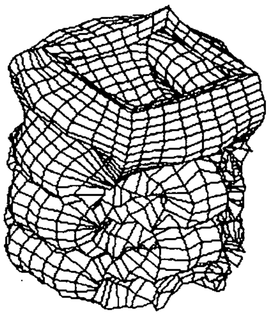

Fig. 10 Simulation of the optimized unstiffened square tube.

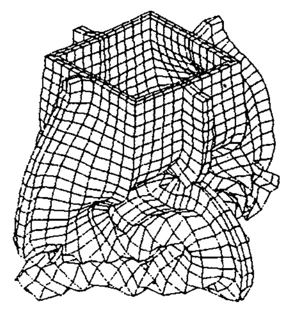

Fig. 11 Simulation of the optimized stiffened square tube.

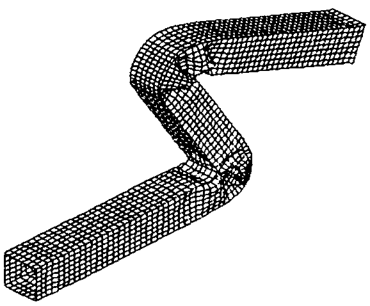

Fig. 12 Simulation of the optimized S-Shape square tube.

square tube, the depth and width of the stiffener are selected as design variables. Both of unstiffeded and stiffened square tubes are known as simple approximations to motor or railway coaches. As the practical application, S-shape square tubes (Fig. 12) which are known as simplified models of front members of an automobile are also optimized. Six dimensions of the mean width and wall thickness of the tube, curvature angle, radius as well as thickness of outer and inner surfaces of curved parts are selected as design variables, and the absorbing energy is maximized under the constraint of axial deformation.

5. Conclusions

The crashworthiness optimization technique for tubular structures was developed and applied to the maximization problem of the crushing energy absorption of tubes. The experiments were also arranged for the validation of the numerical simulation. From the results, it is concluded that the developed optimization technique is applicable and useful for the highly nonlinear structural behavior.

学位論文審査結果の要旨

学位論文審査会は平成11年1月26日に第1回審査会を開催し，論文内容の説明聴取・質疑など一連の審議を慎重に実施した後，平成11年2月2日に行われた口頭発表後に開催した最終審査委員会において協議の結果以下のとおり判定した。

本論文は，動的陽解法有限要素法による薄肉構造部材の軸衝撃圧潰解析モデルの検討と衝撃吸収エネルギに代表される極めて非線形性の強い構造応答の最適設計法の開発とその応用を行ったものである。まず動的陽解法有限要素法による軸衝撃圧潰解析を実施して円筒，リブ無し・リブ付き角筒および曲がり角筒の座屈圧潰現象解析のための寸法比に応じたモデル化法を種々検討すると共にそれらの動的圧潰パターンや衝撃応答を把握して，剛塑性理論による簡易解及び実験結果との比較により数値解析の妥当性を確認している。次にその衝撃圧潰解析法を基礎に実験計画法の直交表を用いた応答曲面近似法と数理計画法を利用した薄肉構造部材の衝撃圧潰エネルギ吸収最大化手法を提案して，与えられた体積制約，圧潰荷重等制約下で円筒，リブ無し・リブ付き角筒及び曲がり角筒の座屈圧潰によるエネルギ吸収量の最大化設計を行い，提案手法の有効性も確認している。また設計結果より，一定質量を持つ円筒や角筒の衝撃力制約下での進行性座屈圧潰では，対称なしわ数を最も多く形成できるような寸法が吸収エネルギ最大寸法を与えることを，またリブはエネルギ吸収時の圧潰変形安定性に寄与すること，さらに曲がり角筒では曲がり部内外周の板厚を補強することでエネルギ吸収を増大できることを見い出している。

以上の成果は，非線形構造最適化分野に大いに貢献するものであり，したがって本論文は博士(工学)の学位に値するものと判定する。